



HAL
open science

XFEL experiments: jitter of pump–probe time delays and pulse intensities

S. Bratos, M. Wulff, J.-Cl. Leicknam

► **To cite this version:**

S. Bratos, M. Wulff, J.-Cl. Leicknam. XFEL experiments: jitter of pump–probe time delays and pulse intensities. *Journal of Synchrotron Radiation*, 2018, 25 (3), pp.650 - 654. 10.1107/S1600577518003624 . hal-01823574

HAL Id: hal-01823574

<https://hal.sorbonne-universite.fr/hal-01823574v1>

Submitted on 26 Jun 2018

HAL is a multi-disciplinary open access archive for the deposit and dissemination of scientific research documents, whether they are published or not. The documents may come from teaching and research institutions in France or abroad, or from public or private research centers.

L'archive ouverte pluridisciplinaire **HAL**, est destinée au dépôt et à la diffusion de documents scientifiques de niveau recherche, publiés ou non, émanant des établissements d'enseignement et de recherche français ou étrangers, des laboratoires publics ou privés.

1 **XFEL EXPERIMENTS:**
2 **JITTER OF PUMP-PROBE TIME DELAYS**
3 **AND PULSE INTENSITIES**

4 S. Bratos¹, M. Wulff², and J-Cl. Leicknam¹

5 *1 - Sorbonne Universités, UPMC Univ Paris 06, Laboratoire Physique Théorique de la*
6 *Matière Condensée, 75005, Paris, France.*

7 *2 - ESRF - European Synchrotron, Complex Systems and Biomedical Sciences (CBS) CS*
8 *40220, 38043 Grenoble Cédex 9, France.*

9
10 **SUMMARY**

11 Jitter of XFEL signals due to fluctuations in shot-to-shot time delays and
12 intensities are explored in the frame of a statistical theory of X-ray diffraction
13 from liquids. Deformed signals are calculated at different levels of pump-probe
14 jitter. A new method is proposed to eliminate these distortions.

16 **I. INTRODUCTION.** Monitoring atomic motions during a chemical reaction
17 has always been an important objective in chemical research. This sort of
18 "filming", inaccessible in the past, can now be realized either by performing
19 time-resolved optical or time-resolved x-ray experiments. Optical experiments,
20 less expensive than x-ray experiments, were realized first and they proved to be
21 highly efficient. The Nobel prize for chemistry was awarded to A. Zewail for his
22 spectacular achievements in this field [1]. However, as the wave length of
23 optical waves are large compared with inter-atomic distances in molecules,
24 optical techniques can not detect atomic positions without complementary
25 assumptions. This difficulty is absent in X-ray experiments. They can be
26 realized, both in diffraction or absorption, either using synchrotron or free
27 electron laser (XFEL) techniques. Pulses of the order of 100 ps can be generated
28 by the former, and 10 fs by the latter. X-ray techniques, in particularly XFEL
29 techniques have proven to be extremely efficient, but a number of difficulties
30 still limit, for the time being, their intrinsic power: the shot-to shot dispersion of
31 pump-probe time delays and of pulse intensities. An important efforts has been
32 made to solve this problem experimentally [2][3][4][5][6][7][8][9]. The recent
33 measure and sort technique [10] merits attention in this context. We complete
34 this effort theoretically by calculating the signal distortions in some typical
35 situations. We also propose a new method to eliminate these distortions..

36

37 **II. THEORY.** (a) In a time-resolved X-ray experiment, the sample is pumped by
 38 an optical pulse and probed by an X-ray pulse. The pump-probe time delay must
 39 be determined with extreme accuracy. At the present time, while XFEL sources
 40 generate pulses down to 10 fs, there is a jitter on the pump-probe time delays of
 41 several hundreds fs. The experiment must thus be repeated and the resulting
 42 signals averaged over this sequence to make the results usable. In this way, a
 43 single-pulse experiment transforms into an multi-pulse experiment. The problem
 44 is thus statistical, not only in its molecular dynamics part, but also in the electric
 45 field part. Statistical mechanics is thus omnipresent, as in ultrafast optical
 46 spectroscopy; see e.g. the text book by Mukamel [11].

47 (b) A statistical theory of x-ray diffraction from liquids was published some time
 48 ago [12]. Its full mathematical development is given in this reference, and will
 49 not be repeated again. Only the essential features are illustrated in what follows.
 50 The intensity of the diffracted x-rays $\Delta S(\mathbf{q}, \tau)$ is:

$$\Delta S(\mathbf{q}, \tau) = \int_{-\infty}^{\infty} dt I_X(t-\tau) \Delta S_{inst}(\mathbf{q}, t)$$

$$\Delta S_{inst}(\mathbf{q}, t) = \left(\frac{e^2}{mc^2\hbar}\right)^2 P \int_0^{\infty} \int_0^{\infty} d\tau_1 d\tau_2 \langle E_i(\mathbf{r}, t-\tau_1) E_j(\mathbf{r}, t-\tau_1-\tau_2) \rangle_O$$

$$\mathbf{x} \langle [[f_m f_n e^{-i\mathbf{q} \cdot \mathbf{r}_{mn}(\tau_1+\tau_2)}, M_i(\tau_2)], M_j(0)] \rangle_S$$
(1)

51 Here P is a factor characteristic of the experimental set-up such as the temporal
 52 pulse profile, polarisation, sample concentration, etc. I_X is the intensity of the
 53 incident X-ray radiation, E_i, E_j are components of the electric field generated by
 54 the optical laser, \mathbf{q} is the wave vector, f_m, f_n are atomic scattering factors, r_{mn} is
 55 the distance between the atoms m and n , and M_i, M_j are components of the laser
 56 induced transition moment M between the states i and j . Einstein's convention
 57 of summing over doubled indices i, j and m, n is employed. The form of this
 58 expression can be understood comparing it with the standard expression for the
 59 diffracted x-ray intensity $S(\mathbf{q}) \sim \sum_{m,n} [f_m \cdot f_n \cdot \exp(-i\mathbf{q} \cdot \mathbf{r}_{mn})]$ [13]. The later is valid if
 60 the incident X ray wave has a constant amplitude and if fast chemical processes
 61 are absent. If the incident X-ray consists of short pulses, and if some fast
 62 chemical process is laser excited, this expression must be modified in two ways.
 63 First, the intensity and the inter-atomic distances r_{mn} are now time dependent,
 64 and I_X and r_{mn} must be replaced by $I_X(t)$ and $r_{mn}(t)$. The remaining quantities in
 65 Eq.(1) describe the laser induced electronic excitation. This can be understood
 66 noticing that, according to the Fermi golden rule, the rate of this excitation is
 67 proportional to $1/\hbar^2(\mathbf{E} \cdot \mathbf{M})^2$, where \mathbf{E} is the laser generated electric field and \mathbf{M}

68 the transition moment. The presence in Eq. (1) of the factors $1/\hbar^2$, $E(t-\tau_1)$, $E(t-\tau_1-$
 69 $\tau_2)$, $M(0)$ and $M(\tau_2)$ can be understood in this way. The connection of different
 70 time points can not be explained as simply. This equation can be used as it
 71 stands when studying single pulse events.

72 Interpreting multi-pulse experiments is more complex, due to the scatter of
 73 pump-probe time delays and shot intensities. However, the form of Eq. (1)
 74 indicates that these problems can be studied independently from those due to
 75 molecular dynamics. Note also that Eq. (1) was conceived for a single pulse
 76 experiment. However, a slight modification makes it applicable to a multi-pulse
 77 experiment: it is sufficient to replace the single X-ray pulse intensity $I_X(t-\tau)$ by
 78 the average multi-pulse intensity $\langle I_X(t-\tau) \rangle_{MP}$, the index MP indicating multi-
 79 pulse. One can then write:

$$\Delta S(q, \tau) = \int_{-\infty}^{\infty} dt \langle I_X(t-\tau) \rangle_{MP} \Delta S_{inst}(q, t) \quad (2)$$

80 where $\Delta S_{inst}(q, t)$ is the same as in Eq. (1). In the rest of this paper, the incident
 81 x-ray beam is supposed to be Gaussian:

$$I_X(t-\tau-\delta\tau) = I \exp[-\gamma_X(t-\tau-\delta\tau)^2] \quad (3)$$

82 where τ is the nominal pump-probe time delay, $\delta\tau$ its ill controlled shut-to-shut
 83 time increment and $(1/\gamma_X)^{1/2}$ its temporal width.

84 c) To proceed further, details about the statistical distribution of $\delta\tau$ and I for
 85 subsequent shots are required. The attention of the experimentalists was centered
 86 on this question for years, and still remains an issue. According to the literature
 87 [14], the distribution of pump-probe time delays $P(\delta\tau)$ is Gaussian:

88 $P(\delta\tau) = \sqrt{\beta/\pi} \exp(-\beta(\delta\tau)^2)$. The distribution of shot-to-shot intensities $P(I)$ is
 89 less well known, but according to Eqn(2) it is needed only if the absolute
 90 intensity of the scattered radiation is explored, which is not the case here. Then,
 91 inserting Eqn(3) into Eqn(2) and integrating over $\delta\tau$, there results:

$$\Delta S(q, \tau) = I \left(\frac{\beta}{\beta + \gamma_X} \right)^{\frac{1}{2}} \int_0^{\infty} dt \exp\left(-\left(\frac{\beta \gamma_X}{\beta + \gamma_X}\right) (t-\tau)^2\right) \Delta S_{inst}(q, t) \quad (4)$$

92 Jitter thus generates an effective temporal broadening of incident x-ray pulses.
 93 This is the basic equation relating the distorted and non-distorted signals
 94 $\Delta S(q, \tau)$ and $\Delta S_{inst}(q, t)$, respectively.

95 To proceed further, the following way can be chosen. Let the laser excitation
 96 promote the molecules from their ground electronic state 0, where the length of
 97 a given bond is r_0 , to an electronic state 1, where it is r_1 . According to the
 98 Franck-Condon principle, $r_1(0) = r_0$ at time $t = 0$. The simplest assumption
 99 to describe the bond length variation at later times consists in writing
 100 $r(t) = r_1 - (r_1 - r_0) \cdot \exp(-t/\tau_r)$ where τ_r is the molecular reaction (or
 101 rearrangement) time (Fig.1). The signal $\Delta S_{inst}(q, t)$, non affected by pump-
 102 probe time delay dispersion, can be written:

$$\Delta S_{inst}(q, t) = \frac{\sin(q(r_1 - (r_1 - r_0) \exp(-t/\tau_r)))}{q(r_1 - (r_1 - r_0) \exp(-t/\tau_r))} - \frac{\sin(qr_0)}{qr_0} \quad (5)$$

103 Then, inserting Eqn(5) into Eqn(4) and integrating provides $\Delta S(q, \tau)$. The
 104 integration can be performed either numerically or analytically if $r_1 - r_0 \ll r_0$.
 105 Note that this condition is not very restrictive. When passing from a single C-C
 106 bond to a triple C-C bond, $r_0 = 1.5\text{\AA}$ and $r_0 - r_1 = 0.3\text{\AA}$. The experimental signal
 107 $\Delta S(q, \tau)$ can then be calculated and its distortion investigated, if the
 108 parameters r_1 and τ_r are known. The opposite problem of extracting the
 109 non perturbed signal $\Delta S_{inst}(q, t)$ from the observed signal $\Delta S(q, \tau)$ is more
 110 difficult. The best is to work with the function $\Delta S(q, \tau)$ in its analytical form:

$$\begin{aligned} \Delta S(q, \tau) \sim & -q(r_1 - r_0) \cdot j_1(qr_0) \\ & \cdot [\operatorname{erfc}(-\sqrt{\frac{\beta \cdot \gamma_x}{\beta + \gamma_x}} \tau) \\ & - \operatorname{erfc}[(\frac{1}{2\tau_r}) \sqrt{\frac{(\beta + \gamma_x)}{\beta \gamma_x}} - \sqrt{\frac{\beta \cdot \gamma_x}{\beta + \gamma_x}} \tau] \exp((\frac{1}{4\tau_r^2}) \frac{\beta + \gamma_x}{\beta \gamma_x} - \frac{\tau}{\tau_r})] \end{aligned} \quad (6)$$

111 where r_0 and r_1 are bond lengths before and after reaction, τ_r is its characteristic
 112 time and $j_1(x)$ is the Bessel function of the order 1 (remember that $\sin x/x$ is the
 113 Bessel function $j_0(x)$). Inserting experimental data into the left hand member of
 114 Eqn(6) then permits to calculate r_1 and τ_r using mean square optimisation
 115 techniques. As there are only two parameters r_1 and τ_r to determine, this
 116 calculation is easy.

117 The corresponding r space signals $\Delta S[r, \tau]$ can be calculated by Fourier
 118 inverting $\Delta S(q, \tau)$. This can be done without any special precaution if τ is
 119 large as compared with the time $\tau < 1/\sqrt{\beta}$ characteristic of pump-probe
 120 dispersion. If this is not the case, $\Delta S(q, \tau)$ must be corrected carrying out the
 121 above procedure for each q, τ point such that $\tau < 1/\sqrt{\beta}$, this making the Fourier
 122 transform possible. It is thus more difficult to correct the signals $\Delta S[r, \tau]$ than
 123 the signals $\Delta S(q, \tau)$.

124 **III. EXAMPLES** (a) Times shorter than the molecular dynamics. Those
 125 considered here are of the order of 10 fs or shorter. At these times a liquid
 126 behaves like a glass. Nevertheless, diffraction signals still vary with time, even if
 127 all inter-atomic distances r are fixed. This is due to the electric fields E_i, E_j of the
 128 optical pump pulses in Eq. (1). The noise of XFEL radiation also plays a major
 129 role. In this limit, one finds :

$$130 \quad \Delta S_{XFEL}(\tau) = Const. \cdot \text{erfc}\left(-\sqrt{\frac{\beta \gamma_x}{\beta + \gamma_x}} \tau\right)$$

131 One concludes that the dispersion of pump probe time delays modifies the
 132 temporal width of the average multi-pulse signals even at very short times.
 133 These effects may be large, even overwhelmingly large; compare with Fig. 2.
 134 Note also that in this short-time limit the q- and r-resolved signals exhibit the
 135 same tau dependence. In fact, in this limit $\Delta S_{inst}(q, t)$ is independent of time. A
 136 look on Eqn(6) then confirms the statement.

137 (b) Contracting chemical bond. In absence of distortion free experimental data in
 138 the 10 - 100 fs time domain, the following example is completely theoretical.
 139 Let us start considering a CC bond contracting from 1.5Å to 1.2Å; these values
 140 correspond to a single and triple CC bond respectively. This CC bond is
 141 supposed to be a part of a polyatomic molecule PolyM. Its CC diffraction peak
 142 is assumed to be sufficiently isolated from other diffraction peaks from PolyM
 143 to be explorable. The laser pump promotes PolyM from its electronic ground
 144 state A, where the CC bond is simple to a state B where it is triple. However,
 145 this transformation is not instantaneous: according to the Franck-Condon
 146 principle, light induced transitions are all vertical. At $\tau = 0$, the CC distance
 147 remains unchanged, equal to 1.5 Å. It is only at later times that it contracts
 148 gradually from 1.5Å to 1.2 Å. How does this contraction process manifests itself
 149 in a r resolved XFEL experiment? And how does this signal deform if the pump-
 150 probe times are dispersed? The central quantities are the pair distribution

151 functions $g(r, t)$; see the textbook [Hansen,1997]. The following expressions are
 152 chosen in our model:

$$g_A = \sqrt{a_A/\pi} \exp[-a_A(r-r_A)^2] \quad (7 \text{ a,b})$$

$$g_B(r, t) = \sqrt{a_B/\pi} \exp[-a_B(r - r_B - \delta r_B \exp(-t/\tau_v))^2]$$

$$n_A(t) = 1 - n_0 \cdot \exp(-t/\tau_p) \quad (8 \text{ a,b})$$

$$n_B(t) = n_0 \cdot \exp(-t/\tau_p)$$

153 Note that $g_A(r)$ and $g_B(r,t)$ approach a delta function when a_A et a_B go to infinity.
 154 Equation (7b) states that the CC bond contracts in the state B of PolyM in times
 155 of the order of τ_v . Employing the above equations together with Eqs. (2, 4)
 156 generates the r -resolved signal $\Delta S(r, \tau)$.
 157 The parameters of the above model are: the ground state distance r_A is 1.5Å and
 158 the excited states distance r_B 1.2Å; the laser induced contraction of the CC bond
 159 in the state B of PolyM is 0.3 Å. The parameters a_A and a_B are both of the order
 160 of 25 \AA^{-2} , which corresponds to a half width of $g_A(r)$ and $g_B(r, t)$ of the order of
 161 0.4 Å. Moreover, the recombination time τ_v is assumed to be of the order of 100
 162 fs, and the population relaxation time $\tau_p \gg \tau$. These values correspond to an
 163 ultrafast chemical process.

164 The results are presented now. Fig. 3a illustrates $\Delta S[r, \tau]$, the r -resolved XFEL
 165 signal of a contracting CC bond in absence of pump-probe time dispersion. This
 166 signal is presented in three dimensions: the distance r and the time τ are defined
 167 on the two coordinate axes while the intensity is given by color. The red valley
 168 at 1.5Å pictures the deficit of CC bonds at the initial bond length of 1.5 Å,
 169 whereas the violet ridge indicates CC bonds of given length r at a given time τ .
 170 Note that the intensity of the differential signal is vanishing at $\tau = 0$: according
 171 to the Frank-Condon principle electronic transitions are vertical. At times
 172 $\tau \sim 10$ fs, intramolecular dynamics of PolyM intervene noticeably. It is only at
 173 times $\tau > 20$ fs that chemistry manifests itself predominantly. The signal
 174 represents a film of a contracting CC bond. If pump-probe times are dispersed,
 175 the above picture is slightly or deeply modified; see Fig. 3b $\Delta S[r, \tau]$ is only
 176 blurred. It is only blurred if the pump-probe time dispersion is small. If the
 177 pump-probe time dispersion is not sufficiently small, the CC contraction is no
 178 longer observable and only an instantaneous jump between the initial and final

179 configurations is observed . This effect is widely known in other fields of
 180 physics and chemistry under the name of motional narrowing.

181 So much for r-resolved signals $\Delta S[r, \tau]$. Let us now pass to the q-resolved
 182 signals $\Delta S(q, \tau)$. The latter can be deduced from $\Delta S[r, \tau]$ using the well known
 183 formula $\Delta S(q, t) = 4\pi/q \int_{-\infty}^{+\infty} dr r \Delta S[r, t] \sin(qr)$ which, according to the basic
 184 theory of x-ray diffraction, relates r-resolved and q-resolved signals
 185 [Warren,2005]. It is valid independently of whether pump-probe time delays
 186 are dispersed or not. This integration was accomplished numerically. The results
 187 are presented in Figs. 4. In Fig. 4a, the signal is calculated for $\beta = \text{infinite}$, i.e. in
 188 absence of pump-probe dispersion . It is presented in three dimensions: the
 189 variables q and τ are placed on the coordinate axes, whereas the value of the
 190 signal $\Delta S(q, \tau)$ is indicated by color. The violet crests indicate the increase of
 191 the signal intensity and the red valleys their decrease. The bending of the red
 192 crests toward large q 's indicates progressive CC contraction from 1.5Å to 1.2
 193 Å. This signal is strictly vanishing at $\tau = 0$, whatever q , which is a
 194 consequence of the Franck-Condon principle. At long times, $\Delta S(q, \tau)$
 195 approaches the limit $Const(r_1^2 \sin(qr_1)/qr_1 - r_0^2 \sin(qr_0)/qr_0)$ (Fig.4b). Atomic
 196 motions during a chemical reaction can thus be monitored in this way.
 197 Nevertheless, visualizing atomic motions is much more difficult in q-resolved
 198 than in r-resolved signals. Fig. 4b pictures this signal in presence of appreciable
 199 pump-probe time dispersion. Only immutable red and violet crest are now
 200 visible, molecular dynamics can no longer be followed. Motional narrowing is
 201 dominating.

202 **IV. CONCLUSION.** Fluctuations of a multi-pulse signal due to of shot-to-shot
 203 variations in time delays and intensities are explored theoretically in the frame
 204 of a statistical theory of X-ray diffraction of liquids. A new method is also
 205 proposed to eliminate the effect of time delay jitter in XFEL experiments.
 206 Contrary to the measure and sort method which is fully experimental, the
 207 present method belongs to the ensemble of signal treatment methods. It does not
 208 require any extra experiment.

209

210 Bibliography

- 1: A. H. Zewail, Femtochemistry. Past, present, and future, *Pure and Applied Chemistry*, (2000) 2219-2231.
- 2: M. Meyer, D. Cubaynes, P. O’Keeffe, H. Luna, P. Yeates, E. T. Kennedy, J. T. Costello, P. Orr, R. Taïeb, A. Maquet, S. Düsterer, P. Radcliffe, H. Redlin, A. Azima, W. Li, E. Plönjes, and J. Feldhaus, Twocolor photoionization in xuv freeelectron and visible laser fields, *Phys. Rev. A*, (2006) 011401.
- 3: D. M. Fritz, D. A. Reis, B. Adams, R. A. Akre, J. Arthur, C. Blome, P. H. Bucksbaum, A. L. Cavalieri, S. Engemann, S. Fahy, R. W. Falcone, P. H. Fuoss, K. J. Gaffney, M. J. George, J. Hajdu, M. P. Hertlein, P. B. Hillyard, M. Horn-von Hoegen, M. Kammler, J. Kaspar, R. Kienberger, P. Krejcik, S. H. Lee, A. M. Lindenberg, B. McFarland, D. Meyer, T. Montagne, É. D. Murray, A. J. Nelson, M. Nicoul. Pahl, J. Rudati, H. Schlarb, D. P. Siddons, K. Sokolowski-Tinten, Th. Tschentscher, D. von der Linde, J. B. Hastings, Ultrafast Bond Softening in Bismuth: Mapping a Solid's Interatomic Potential with X-rays, *Science*, (2007) 633-636.
- 4: T. Maltezopoulos, S. Cunovic, M. Wieland, M. Beye, A. Azima, H. Redlin, M. Krikunova, R. Kalms, U. Frühling, F. Budzyn, Single-shot timing measurement of extreme-ultraviolet free-electron laser pulses, *New Journal of Physics*, (2008) 033026.
- 5: A. Azima, S. Düsterer, P. Radcliffe, H. Redlin, N. Stojanovic, W. Li, H. Schlarb, J. Feldhaus, D. Cubaynes, M. Meyer, J. Dardis, P. Hayden, P. Hough, V Richardson, E. T. Kennedy, and J. T. Costello, Time-resolved pump-probe experiments beyond the jitter limitations at FLASH, *Applied Physics Letters*, (2009) 144102.
- 6: J. M. Glowia, J. Cryan, J. Andreasson, A. Belkacem, N. Berrah, C. I. Baga, C. Bostedt, J. Bozek, L. F. DiMauro, L. Fang, J. Frisch, O. Gessner, M. Gühr, J. Hajdu, M. P. Hertlein, M. Hoener, G. Huang, O. Kornilov, J. P. Marangos, A. M. March, B. K. McFarland, H. Merdji, V. S. Petrovic, C. Raman, D. Ray, D. A. Reis, M. Trigo, J. L. White, W. White, R. Wilcox, L. Young, R. N. Coffee, and P. H. Bucksbaum, Time-resolved pump-probe experiments at the LCLS, *Optics Express*, (2010) 17620-17630.
- 7: F. Löhl, V. Arsov, M. Felber, K. Hacker, W. Jalmuzna, B. Lorbeer, F. Ludwig, K.-H. Matthiesen, H. Schlarb, B. Schmidt, P. Schmöser, S. Schulz, J. Szewinski, A. Winter, and J. Zemella, Electron Bunch Timing with Femtosecond Precision in a Superconducting Free-Electron Laser, *Phys. Rev. Lett.*, (2010) 144801.
- 8: Bionta, Mina R.; Lemke, H. T.; Cryan, J. P.; Glowia, J. M.; Bostedt, C.; Cammarata, M.; Castagna, J.-C.; Ding, Y.; Fritz, D. M.; Fry, A. R.; Krzywinski, J.; Messerschmidt, M.; Schorb, S.; Swiggers, M. L.; Coffee, R. N., Spectral encoding of x-ray/optical relative delay, *Optics Express* 10, (2011) 21855-21865.
- 9: F. Tavella, N. Stojanovic, G. Geloni & M. Gensch, Few-femtosecond timing at fourth-generation X-ray light sources, *Nature Photonics*, (2011) 162-165.

10: M. Harmand, R. Coffee, M. R. Bionta, M. Chollet, D. French, D. Zhu, D. M. Fritz, H.T. Lemke, N. Medvedev, B. Ziaja, S. Toleikis, M. Cammarata, Achieving few-femtosecond time-sorting at hard X-ray free-electron lasers, *Nature Photonics*, (2013) 215–218.

11: S. Mukamel, Principles of Nonlinear Optics and Spectroscopy, 1995

12: S. Bratos, F. Mirloup, R. Vuilleumier and M. Wulff, Time-resolved x-ray diffraction: Statistical theory and its application to the photo-physics of molecular iodine, *J. Chem. Phys.*, (2002) 10615.

13: B.E. Warren, X-Ray Diffraction, 1990

14: Cavalieri, A. L., Fritz, D. M., Lee, S. H., Bucksbaum, P. H., Reis, D. A., Rudati, J., Mills, D. M., Fuoss, P. H., Stephenson, G. B., Kao, C. C., Siddons, D. P., Lowney, D. P., MacPhee, A. G., Weinstein, D., Falcone, R. W., Pahl, R., Als-Nielsen, J., Blome, C., Dusterer, S., Ischebeck, R., Schlarb, H., Schulte-Schrepping, H., Tschentscher, Th., Schneider, J., Hignette, O., Sette, F., Sokolowski-Tinten, K., Chapman, H. N., Lee, R. W., Hansen, T. N., Synnergren, O., Larsson, J., Techert, S., Sheppard, J., Wark, J. S., Bergh, M., Caleman, C., Huldt, G., van der Spoel, D., Timneanu, N., Hajdu, J., Akre, R. A., Bong, E., Emma, P., Krejcik, P., Arthur, J., Brennan, S., Gaffney, K. J., Lindenberg, A. M., Luening, K., Hastings, J. B., Clocking Femtosecond X Rays, *Phys. Rev. Lett.*, (2005) 114801.

15: P.A. Janson, Deconvolution of Images and Spectra, 1997

16: J.P. Hansen and I.R.M Mac Donald, Theory of Simple Liquids, 2006

211

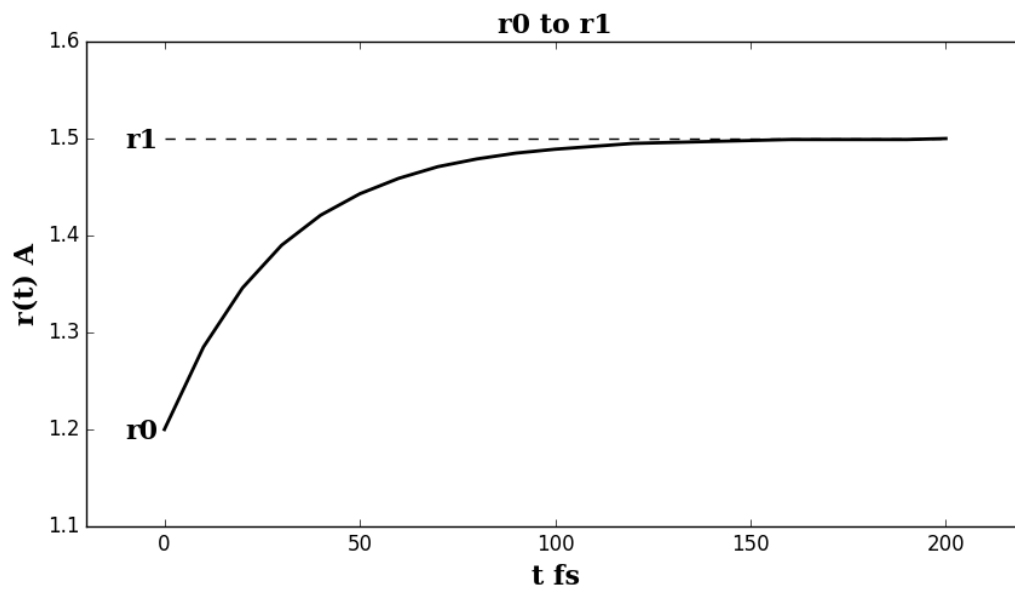
212

213

214

215

216

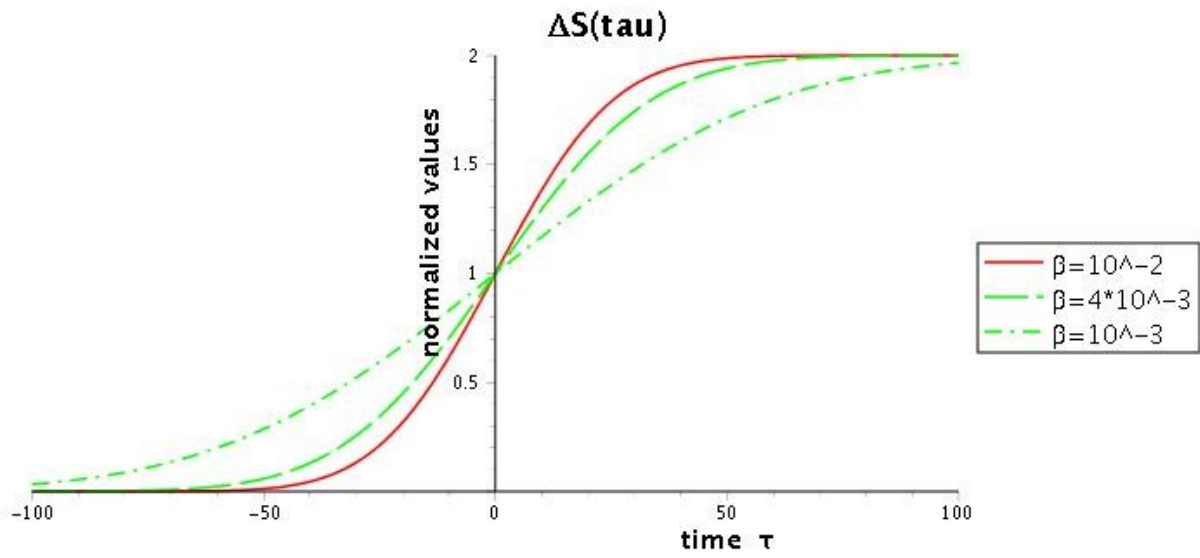


218 Fig. 1: Variation of the bond length $r(t)$ from r_0 to the laser excited state r_1 .

219

220

221



223 Fig. 2: Variation of ΔS at shortest pump-probe times delays.

224

225

226

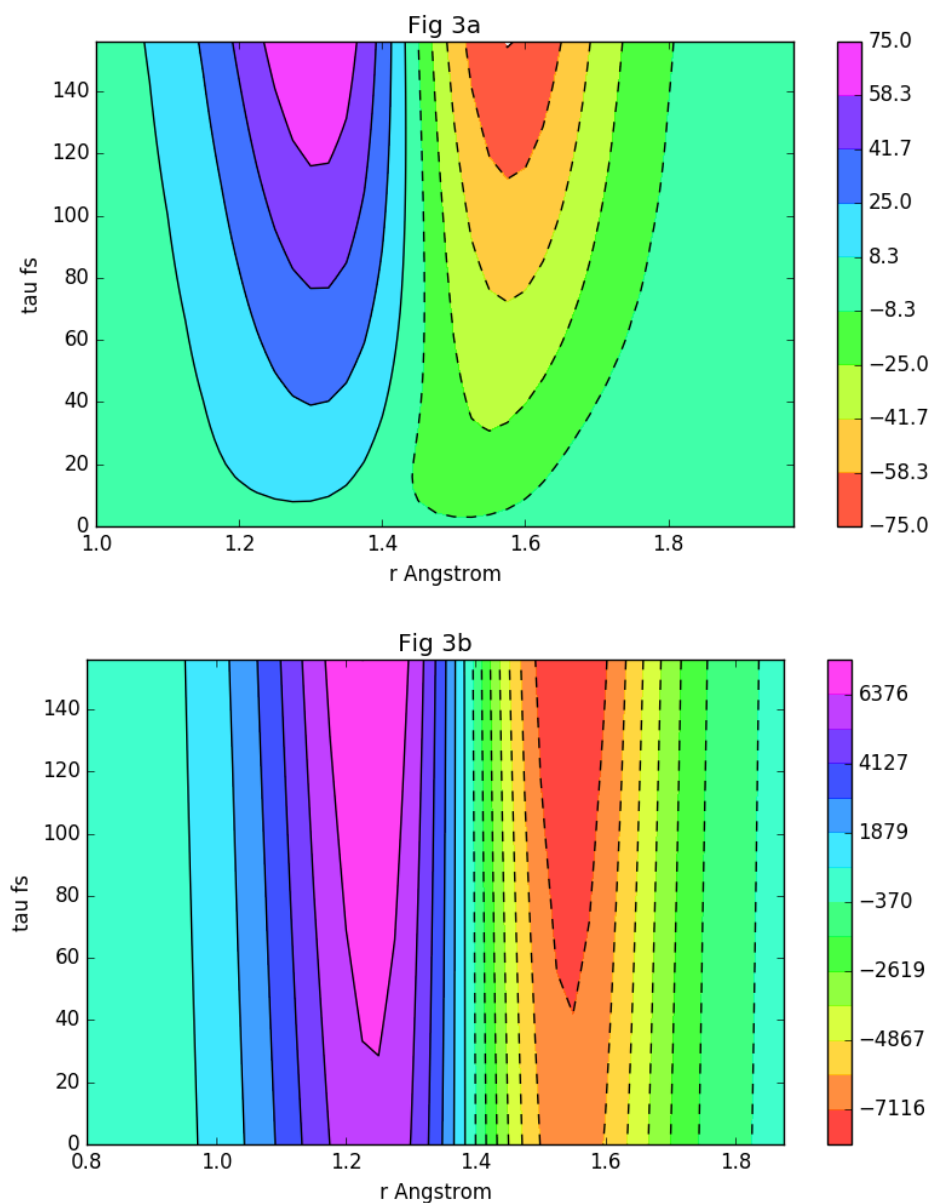
227 :

228

229

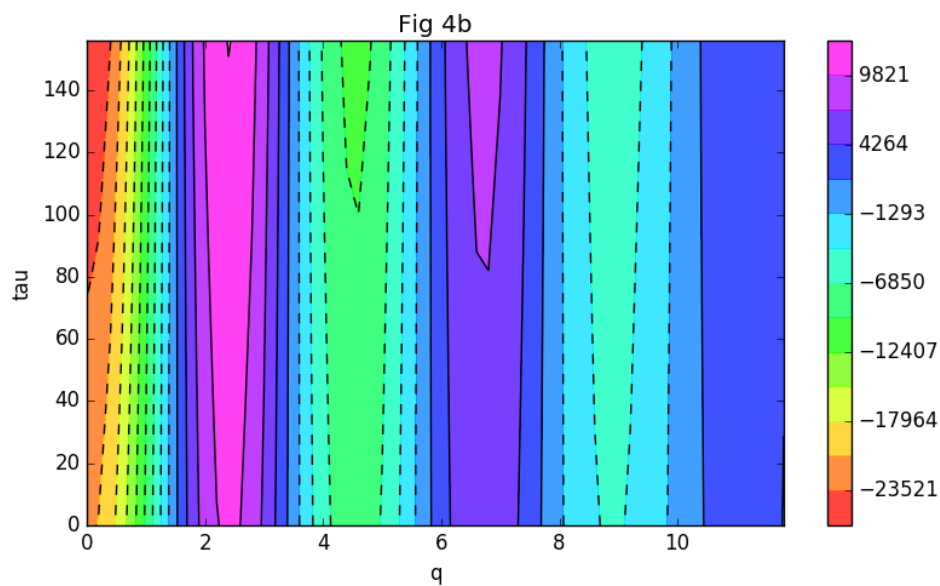
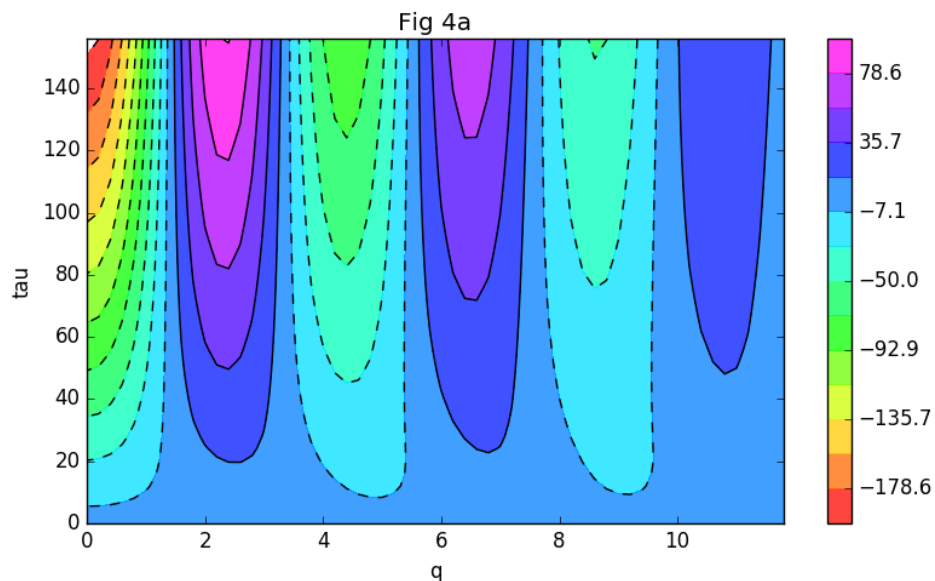
230

231



233

234 Fig. 3: Contraction of the CC bond after laser excitation: multi-pulse signal in r
 235 space. The CC bond contracts from the single bond length (1.5 Å) to the triple
 236 bond length (1.2 Å). The process is supposed to be accomplished in 100 fs. (a)
 237 The signal $\Delta S(r, \tau)$ in absence of pump-probe time delay dispersion, (b) in its
 238 presence (1000 fs). The contraction of the CC bond is clearly visible in Fig. (a),
 239 but is not in Fig. (b).



242 Fig. 4: Contraction of a CC bond after laser excitation: the multi-pulse signal in
 243 q space. This signal is defined as the difference of multi-pulse signals $S(q, \tau)$ in
 244 presence or absence of pump-probe time delay dispersion. Time-delay
 245 dispersion is supposed to be of the order of 1000 fs. The contraction is no
 246 longer perceptible at this level of jitter.

247